

---

This is an electronic reprint of the original article.  
This reprint may differ from the original in pagination and typographic detail.

Anwar, Nurul; Jalava, Kalle; Orkas, Juhani

## Experimental Study of Inorganic Foundry Sand Binders for Mold and Cast Quality

*Published in:*  
International Journal of Metalcasting

*DOI:*  
[10.1007/s40962-022-00897-4](https://doi.org/10.1007/s40962-022-00897-4)

Published: 01/07/2023

*Document Version*  
Publisher's PDF, also known as Version of record

*Published under the following license:*  
CC BY

*Please cite the original version:*  
Anwar, N., Jalava, K., & Orkas, J. (2023). Experimental Study of Inorganic Foundry Sand Binders for Mold and Cast Quality. *International Journal of Metalcasting*, 17(3), 1697-1714. <https://doi.org/10.1007/s40962-022-00897-4>

---

This material is protected by copyright and other intellectual property rights, and duplication or sale of all or part of any of the repository collections is not permitted, except that material may be duplicated by you for your research use or educational purposes in electronic or print form. You must obtain permission for any other use. Electronic or print copies may not be offered, whether for sale or otherwise to anyone who is not an authorised user.

# EXPERIMENTAL STUDY OF INORGANIC FOUNDRY SAND BINDERS FOR MOLD AND CAST QUALITY

Nurul Anwar , Kalle Jalava  and Juhani Orkas 

Department of Mechanical Engineering, Aalto University, Puumiehenkuja 3, 02150 Espoo, Finland

Copyright © 2022 The Author(s)  
<https://doi.org/10.1007/s40962-022-00897-4>

## Abstract

*The interest in inorganic foundry binders has been rising steadily in recent times due to their favorable environmental characteristics. This paper compares the mold quality and cast quality attained with different inorganic binders. Three different types of sand and five different inorganic binders were used for the mold quality study. Of the inorganic binders, there was liquid sodium silicate used in different hardening methods, a geopolymer binder, and also solid sodium silicate. The mold quality was assessed through bending strength, residual bending strength, tensile strength, and loss on ignition measurement. A total of*

*12 castings were made using molds of different binders and sand materials. The cast quality was then assessed by tracking changes in dimension and the surface quality of final castings. Inorganic binders performed well in terms of mold strength and very well in terms of loss on ignition but there is room for improvement in the surface quality of the castings attained.*

**Keywords:** metal casting, inorganic binder, solid silicate, geopolymer, cast quality

## Introduction

### The 'Renaissance' of Inorganic Binders

Inorganic sodium silicate binders have been used in foundries since mid-twentieth century (Ch. 1).<sup>1</sup> However, due to certain challenges these binders have had, their use and popularity have been limited. Some of the challenges of inorganic binders include poor knock-out performance compared to organic binders, susceptibility to moisture, difficulty with reclamation, need for heat or CO<sub>2</sub> for hardening, etc. (p. 219)<sup>2</sup> (p. 204).<sup>3</sup> These challenges have contributed to organic binders gaining popularity. The advantages of chemical no-bake organic binders in terms of their ease of use, good mold quality, more process reliability, and efficient sand reclamation made them popular for foundry use (Ch. 2).<sup>1,4,5</sup> But in recent times, strong drive toward more sustainable manufacturing has emerged. Concerns are raised over volatile organic compounds (VOCs) which are emitted at elevated temperatures due to

thermal breakdown of organic binders.<sup>5</sup> Many researches were focused on the quality of acid hardeners used with organic binders, which were found to strongly affect emission of the harmful gases.<sup>6,7</sup> Apart from the emissions, the concern over some of the organic binders being classified as possible carcinogen<sup>8</sup> is driving a major interest in inorganic sodium silicate binders. Such binders produce little to no fumes during pour and do not emit any toxic substances, no unpleasant smells either (p. 219)<sup>2</sup> (p. 204).<sup>3</sup> Along with reduced health hazards, foundries can also benefit economically as inorganic binders cost less than organic binders (p. 219).<sup>2</sup> There could also be savings in ventilation systems, as the absence of detrimental casting fumes and binder aerosols mean that less investment is needed in air purification and exhaust equipment.<sup>9,10</sup> Inorganic cores used in die casting also cause less tool contamination, hence less time is required in the cleaning of the dies. More recently, modified version of silicate binder was successfully used in the casting of critical automotive parts.<sup>9</sup> Some steel foundries also take advantage of the fact that, with the use of silicate binder, facing molds with chromite sand is not necessary. As free water and water of crystallization are removed from sodium silicate binder, a considerable amount of latent heat is transferred out, in a similar fashion when good heat

**Supplementary Information** The online version contains supplementary material available at <https://doi.org/10.1007/s40962-022-00897-4>.

Received: 23 May 2022 / Accepted: 21 September 2022 /  
Published online: 8 October 2022

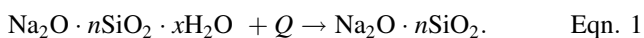
conducting chromite sand is used as facing sand for the same purpose (p. 938).<sup>11</sup> Interest is also growing in other types of inorganic binders, for example, alkaline aluminosilicates, more commonly termed as geopolymers.

Progress toward sustainable manufacturing is a global trend, driven in part by stricter environmental protection laws. Inorganic binders are potential solutions for achieving sustainability. This renaissance of sodium silicate leads to foundries considering switching binder systems needing data how comparable everything is in terms of mold and casting quality.

### Sodium Silicate Hardening Mechanism

Sodium silicate of module 2–2.9 is most often used in foundry industry (p. 225).<sup>2</sup> This module (also known as molar ratio), is the ratio of number of moles of silicon dioxide (SiO<sub>2</sub>) to that of sodium oxide (Na<sub>2</sub>O). A higher module means higher viscosity at same density (p. 225).<sup>2</sup> Usual binder addition rate varies between 2 and 4% by mass of sand (Ch. 9).<sup>2</sup> Sodium silicate hardening is usually of two types, irreversible and reversible. Irreversible hardening occurs through chemical means, by application of CO<sub>2</sub> or a mixture of esters. The reversible hardening occurs by physical hardening through dehydration. This is achieved through furnace or microwave heating.

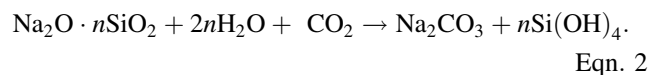
When heat is supplied to sodium silicate, water is lost, turning the silicate into an anhydrous glassy film joining matrix grains together. This process is reversible, which is why moisture can affect heat-hardened mold and core negatively during the storage.<sup>9</sup> As the process is slow,<sup>9</sup> molds in this process suffer from weak initial strength and long cycle times; consuming time, energy, and thus money. In addition, uniformly heating large molds properly is a challenge on its' own. On top of these, collapsibility issues and poor reclamation of sodium silicate remain. Microwave heating, another variant of heat-hardened sodium silicate, offers good mechanical properties of the mold already at 1.5% addition,<sup>12</sup> and low binder addition in turn offers better reclamation and collapsibility.<sup>13</sup> It was shown in<sup>13</sup> that, unit costs for cores could be reduced with microwave hardening for mass production compared to furnace heating. The heat-hardened reaction is shown in stoichiometric Eqn. 1 (p. 230)<sup>2</sup>.



Using esters to harden sodium silicate results in a hybrid semi-inorganic system. Hydrolysis of ester forms acetic acid, while the acetic acid dissociates to form acetic anions. The acetic anions then react with sodium silicate to form gel. Hydrated sodium acetate, which is formed in this process, hinders both wet and dry reclamation of sodium silicate molding sands.<sup>14,15</sup> Weak initial strengths and

issues of collapsibility are also major drawbacks of this system. However, the system requires the use of less sodium silicate (2–3%) and hardening rates can be adjusted by using different blends of esters (p. 227).<sup>2</sup> The system is self-setting, hence an obvious advantage as no heat or gas is required. The esters are usually glycerol diacetate, ethylene glycol diacetate, or glycerol triacetate depending on what speed of cure is desired, sometimes a blend of esters is also used (p. 211).<sup>3</sup>

For hardening sodium silicate with CO<sub>2</sub>, there should be enough permeability to allow the gas to pass through properly. Due to this, molds cannot be compacted like with other binders. Therefore, it means that the theoretical maximum strength of molds is never reached. In addition, there are issues with flowability, bad reclamation properties, long cycle times, poor storability of cores, etc. The stoichiometric reaction of sodium silicate binders with carbon dioxide is given in Eqn. 2.<sup>16</sup>



### Sodium Silicate Modification

Physical and chemical modifications are being done to sodium silicate to overcome the challenges originally faced with this type of binder. Physical modification involves tuning of temperature and conditioning time of silicate sodium glaze, the primary material (p. 234).<sup>2</sup> Chemical modifications are achieved through introduction of different chemicals into the polymer matrix. These include morphoactive organic compounds (containing functional groups like –OH, –NH<sub>2</sub>, =CONH, –COOH, etc.), ultrafine powders from aluminosilicates (consisting of ions like Mg<sup>2+</sup> and Al<sup>3+</sup>), and nanoparticles of metal oxides (ZnO, MgO, Al<sub>2</sub>O<sub>3</sub>) in various alcoholic solutions (pp. 235–236).<sup>2</sup> The introduction of nanoparticles creates new systems known as nanocomposites, which modifies the properties of the binder in the interface layers, improving mechanical and thermal properties of the binder.<sup>17</sup> Tensile strength, flowability, and collapsibility behavior of sodium silicate bonded core was shown to be improved through the addition of potassium hydroxide, sodium hexametaphosphate, and white sugar modifiers in.<sup>18</sup>

Commercial brands of heat-hardened sodium silicate binders also exist that come in the form of a modified sodium silicate binder and a solid promoter as second component of the binder. The hardening being a combination of physical and chemical reaction means that it improves many parameters like flowability and resistance to atmospheric moisture. Some modified sodium silicate binders have already been successfully used in the production of cores with complex geometries that are used in the

production of high-volume production of castings like aluminum engine cylinder heads and blocks.<sup>9</sup>

### Solid Powder Form of the Silicate Binder

Recently, there have been trials and discussion on using a powder form of sodium silicate rather than any liquid form. The differences in strength properties of silica molds made with powder silicates, liquid silicates, and modified liquid silicates were investigated in.<sup>19</sup> In addition, some 3D printing parameters and effect of boron compounds and microsilica were also investigated. Use of silicate powders instead of liquid silicates reduces manufacturing costs of molds and reduces the cost of handling, storage, and transportation<sup>19</sup> as an equivalent powder form weighs significantly less than liquid silicate binders. Also, the possibility of using powder silicates opens new possibilities in 3D printing of sand molds. In many conventional three-dimensional printing methods, sand is premixed with an activator or hardener, while binder is jetted selectively through inkjet depositors. However, for this process to work optimally, the binders must be modified so that they can be jetted through the printheads. Thus, issues like clogging of nozzles arise. If powder silicate binders are used, powder can be premixed with sand and only thickened water is jetted through the printhead, simplifying the jetting process.<sup>20</sup> Dried silicate-coated sand can also be used in the same process. The dry silicate dissolves and becomes activated in the regions where water is jetted, starting polymer formation. Hardening can be achieved by physical dehydration through heating or microwaving. In,<sup>20</sup> a controllable IR emitter was used to harden the binder.

### Geopolymers

Geopolymers belong to the group of alkaline aluminosilicates and are inorganic materials. The polymers contain chains of  $\text{SiO}_4$  and  $\text{AlO}_4$  tetrahedrons and by altering the ratio of Si:Al, properties of binder system could be altered [1, Sec. 3.4]. Binders currently in use have Si:Al ratio of about 10:1<sup>21</sup>. Geopolymers are not formed by geological processes but are manufactured artificially from slag or fly ashes. The name comes from the fact that their composition is close to that of natural rocks.<sup>22</sup> The binder is already a polymer with low degree of polymerization, while polymerization increases during the hardening reaction.<sup>23</sup> Currently, geopolymer binders are hardened by one of three ways. Self-hardening mixtures, hardened by gaseous carbon dioxide for both mold and cores or hot box technology for cores only (p. 278).<sup>2</sup> Geopolymer binders achieve high strength, good flowability, and permeability.<sup>24</sup> These also exhibit better collapsibility and sand reclamation compared to sodium silicate (p. 278).<sup>2</sup> Gases produced are mainly water vapor, with no hazardous fumes or unpleasant smells.<sup>25</sup> Reduced gas emission also reduces

gas defects in castings. Due to these favorable characteristics, the interest in geopolymers for foundry use is rising.

### Purpose of this Study

With time, it is becoming increasingly likely that the use of inorganic binders is going to increase as all manufacturing industries, including metal casting, are moving toward more sustainable processes. Many foundries are considering or researching their switch to inorganic binders. This study explores how the different forms of inorganic binders introduced compare against each other. Mold quality parameters are experimented with different forms of inorganic binders and three types of sand. Due to the potential solid silicates hold both for normal foundry use and for three-dimensional printing, special consideration is given to the powder sodium silicate. In literature, studies explore mold characteristics of solid silicates as explained in Section “[Solid Powder Form of the Silicate Binder](#)”. However, casting trials including them are rare. This study includes casting trials with several different types of inorganic binders. Unmodified sodium silicate and esters are used in the study as well as some commercial types optimized for foundry use. Unmodified sodium silicate aid in comparison of the solid silicates. In addition, commercial brands of current state-of-the-art organic binders are incorporated in some parts of the study ensuring a better comparison. Figure 1 visualizes the experimental process followed in this study while the details are given in Section “[Material and Methods](#)”.

### Material and Methods

#### Material

The principal type of sand used in the study is silica ( $\text{SiO}_2 > 98\%$ ), while some tests were carried out using sintered Bauxite ( $\text{Al}_2\text{O}_3$ : 74.2%,  $\text{Fe}_2\text{O}_3$ : 15.2%,  $\text{SiO}_2$ : 5.7%) and Cerabeads 400 (Short form: CB 400;  $\text{Al}_2\text{O}_3$ : : 60–62%,  $\text{SiO}_2$  : 36–38%). Five different forms of inorganic binders (Binders A to E) were used for the mold study. The content of the sand and binder mixture for each type is given in Table 1. The values given are used for 1700g of silica sand. Sieve analysis and base permeability test was performed on the sand types used in the study. Organic binders F and G were not used for the mold study but were used for the casting trial to better understand how casting with inorganic binders compares with the organic ones. The reader is referred to<sup>26</sup> for information on mold quality involving organic binders.

For sintered Bauxite and CB 400, the same amount of binder is used. Same volume of sintered Bauxite and CB 400 is used to ensure equal amount of binder per unit volume of sand. It was found in<sup>26</sup> that binder type does not

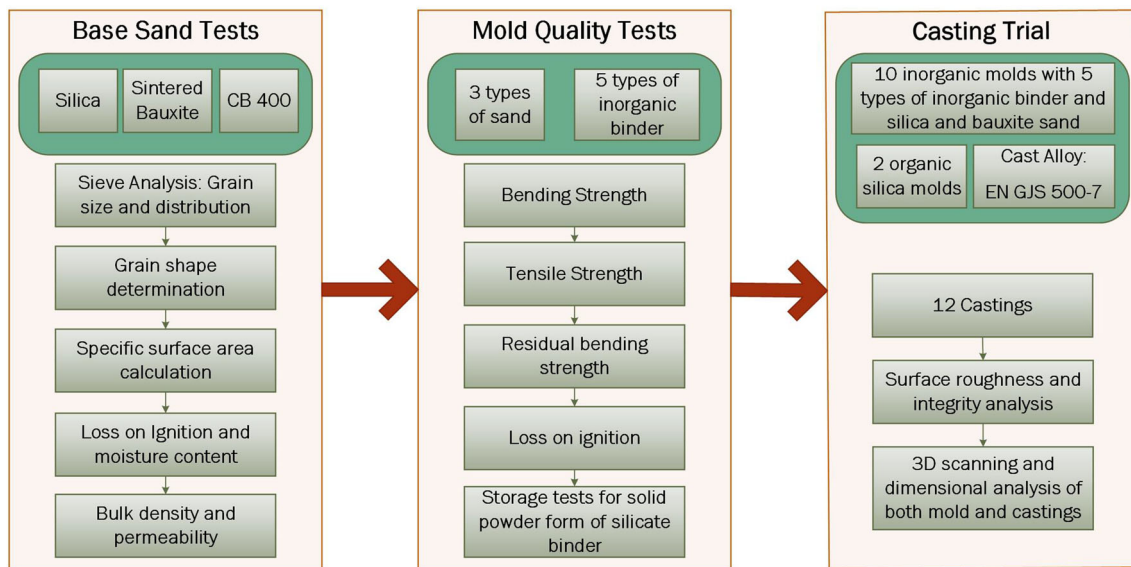


**Figure 1. Experimental process flowchart.**

influence mold permeability much. Instead, it is the sand type which influences permeability more. Hence, in this study only base permeability of the sand was measured using Simpson Digital Absolute Permmeter. The mean particle size and specific surface area of the sands were calculated after sieve analysis and bulk density was measured. Grain shape was determined according to test procedure AFS 1107-12-S.<sup>27</sup> Moisture content according to test procedure AFS 2219-00-S.<sup>27</sup> For estimating the specific surface area of the sands, grain shape factors were used from test procedure AFS 1109-12-S,<sup>27</sup> after calculating the theoretical specific surface area using sieve analysis results and equation 4 in (p. 15)<sup>28</sup> and true density values of sands from (Ch. 5)<sup>1</sup>.

### Strength and LOI Values

Strength and loss on ignition (LOI) values were measured from the test bars. For each sand and binder combination, three bending strength test bars were made (measuring 172mm in length and 22.4 mm × 22.4 mm in cross section), and one dog bone specimen was made for tensile strength measurement. For the heat-hardened binders, the strength was measured after heating the test bars to 160 °C for 1 hour. For others that did not require any heat, the bending strength was measured after 24h. This allowed sufficient time for final hardening and ensures a fair comparison. To analyze the thermal and collapsibility behavior of the different binders containing sand molds, residual bending strength was measured at 160 °C, 450 °C, and 900 °C for all binder types. These test bars were heated for 30 minutes before measuring the bending strength. For powder silicates (Binder E), their storage in mixed form with silica sand is also evaluated. This was done by mixing powder silicate and silica sand and storing them for a

particular time, some in closed plastic container and some open to air. After the intended storage time, the mixture is taken out, water is added, and test bars were made to measure the strengths. A universal strength tester was used for both bending strength and tensile strength measurements. Only one reading was taken for tensile strength, this was an additional measurement taken with the excess available sample, intended for no statistical purpose but as additional information. Therefore, no error bars are available for the tensile strength measurements.

The loss on ignition values was measured by cutting pieces out of test bars and heating them to 915 °C for 2h. To ensure comparable results between the different types, all the samples were first heated to 160 °C, as two of the binders were heat-hardened at 160 °C. Then the samples were heated to 915 °C in a muffle furnace. Loss on ignition was then measured as the percentage loss in mass before and after heating it to 915 °C.

### Casting Trials

Casting trials were made with 12 different sand and binder combinations. The pattern used was an aluminum metal pattern as shown in Figure 2. A metal pattern was chosen as some of the molds had to be heated to 160 °C with the pattern inside it. Hence, wooden or most plastic patterns were not compatible in this experiment. One example of the mold made is shown in Figure 3. 12 such small molds were made for 12 different combinations of sand and binder as shown in Table 2. These small molds were then combined into a big silica phenolic mold so that the casting could be done at once as shown in Figure 4. The small molds were stored within plastic packaging before being combined into the large mold. The ambient temperature

**Table 1. Binder Content and Amount Used in the Study**

Name	Description	Binder amount	Hardener/co-reactant	Basis for binder/hardener amount selection
Binder A	Liquid sodium silicate with molar ratio 3.2–3.4. Solid content: 34.1–37.8%	51 g (3% by mass of sand)	Heated to 160 °C	An intermediate of the usual binder addition rate is chosen
Binder B	Binder A cured with a mixture of esters	51 g (3% by mass of sand)	7.65g (15% by mass of binder)	Ester amounts comparable to commercial binders but tuned to get good output
Binder C	Ester-cured sodium silicate. Commercially available type for foundry use	42.5 g (2.5% by mass of sand)	5.1g (12% by mass of binder)	Manufacturer recommendation
Binder D	Ester-cured aluminosilicate, more commonly known as geopolymer. Commercially available type for foundry use. Manufacturer claims up to 100% of reclaimed sand could be used	30.6 g (1.8% by mass of sand)	4.90g (16% by mass of binder)	Manufacturer recommendation
Binder E	Hydrated sodium disilicate powder with molar ratio 2.0. Water content: 16-20%. Particle size: 70µm	14.11g (0.83% by mass of sand)	19.89g (1.17% by mass of sand) of distilled water is used. Then heated to 160 °C for hardening.	According to <sup>19</sup>
Binder F	Alkaline Phenolic binder. Commercially available type used widely in foundry industry	25.5g (1.5% by mass of sand)	6.38g (25% by mass of binder)	Test procedure AFS 3335-04-S <sup>27</sup>
Binder G	Furan. Commercially available type used widely in foundry industry	17g (1% by mass of sand)	5.61g (33% by mass of binder)	Manufacturer recommendation

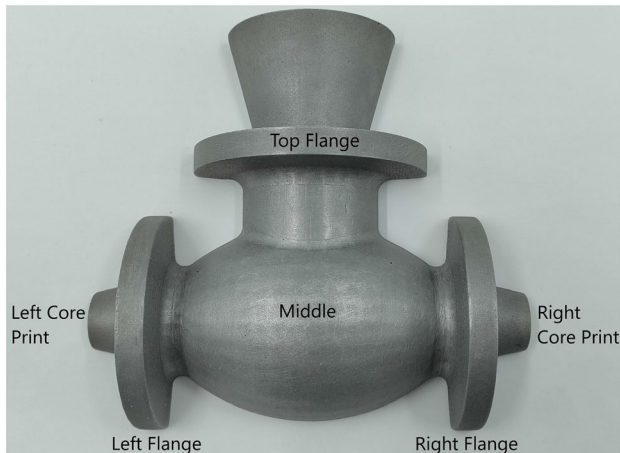


**Figure 2. Pattern used for casting trial.**

during the storage was 20–22 °C, and relative humidity between 56% and 64%. The downsprue was in the middle of the runner seen in Figure 4, and the positions of the mold inserts were documented for later use. Some unintended angling of the inserts can be seen in the molding.



**Figure 3. One mold prepared using silica and Binder C (Sil-C mold).**

Cast alloy used in the casting trial is a general-purpose ferritic–pearlitic ductile iron, EN GJS 500-7. Metal composition of the alloy is shown in Table 3. This type of ductile iron was chosen because used pouring temperatures being in a range not requiring refractory coatings, but of high enough thermal exposure to potentially exhibit issues in mold quality. The pouring temperature of the molds

**Table 2. List of Different Molds Used for Casting Trial**

Combination name	Mold composition		Remarks
	sand	Binder	
Sil-A	Silica	A	Heated to 160 °C for 1 hour
Sil-B	Silica	B	Self-hardening mixture. No heating.
Sil-C	Silica	C	Self-hardening mixture. No heating.
Sil-D	Silica	D	Self-hardening mixture. No heating.
Sil-E	Silica	E	Heated to 160 °C for 1 hour
Sil-E-MR	Silica	E and mold release agent	Mold release agent is sprayed on to the pattern for easier removal of pattern from the mold. Mold is heated to 160 °C for 1 hour.
Sil-F	Silica	F	Self-hardening mixture. No heating.
Sil-G	Silica	G	Self-hardening mixture. No heating.
Bx-A	Sintered Bauxite	A	Heated to 160 °C for 1 hour.
Bx-E	Sintered Bauxite	E	Heated to 160°C for 1 hour.
Sil-Bx-A	Silica and Sintered Bauxite (50% each by volume)	A	Heated to 160 °C for 1 hour.
Sil-Bx-E	Silica and Sintered Bauxite (50% each by volume)	E	Heated to 160 °C for 1 hour.

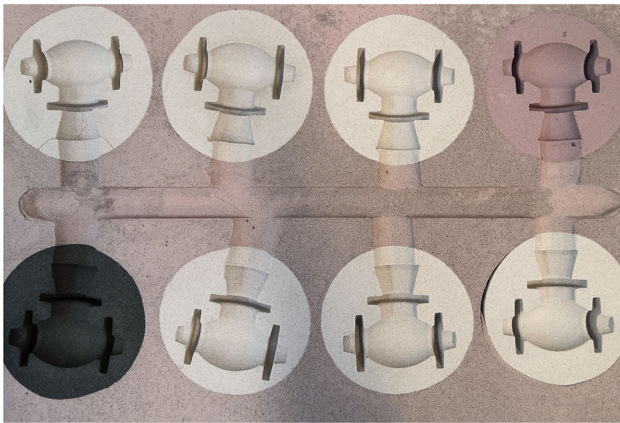


**Figure 4. Small molds combined into a big mold.**

is estimated to be in the range 1380 °C–1420 °C, metal temperature having been measured with an immersion lance at 1420 °C before the start of the pouring run. Combined height of downsprue and pouring basin was 250 mm, the mold cavities being in the drag side of the mold.

### 3D Scans of the Pattern, Molds, and Final Castings

To track each stage of process, 3D scans were taken of the pattern, the molds made and the final castings. The 3D scanner used was based on structured light process, with a claimed accuracy of up to 0.05 mm. From the 3D scans, measurements were made of specific distances and the

**Table 3. Metal Composition (% by wt)**

C	Si	Mn	P	S	Mg	Cu
3.524	2.420	0.304	0.028	0.007	0.064	0.427

changes were documented and analyzed in each stage of the process, from pattern to mold and mold to final castings. Mesh-to-mesh comparisons were also made between pattern 3D scan and final castings 3D scan which shows visual deviations between them. Figure 5 shows a scan of the pattern with some marked measurements which were also measured in the mold and casting scans. It was necessary to use an anti-reflective spray to scan the pattern and most of the castings to overcome the limitation of structured light scanning on shiny metal surfaces.

### Surface Quality

Common methods of assessing as-cast surface conditions include the use of Gar Microfinish comparator C-9 or the SCRATA plate (as per ASTM A802 standard).<sup>29,30</sup> The operator visually compares castings with these reference plates, therefore offering only discrete assessment levels. It is also very difficult to distinguish between two surfaces which have close surface roughness. In literature, there are also suggestions of using point clouds from 3D scans to analyze surface quality of the whole castings rather than a small representative surface.<sup>31</sup> However, for the purpose of the current study, the use of a 3D optical profilometer was

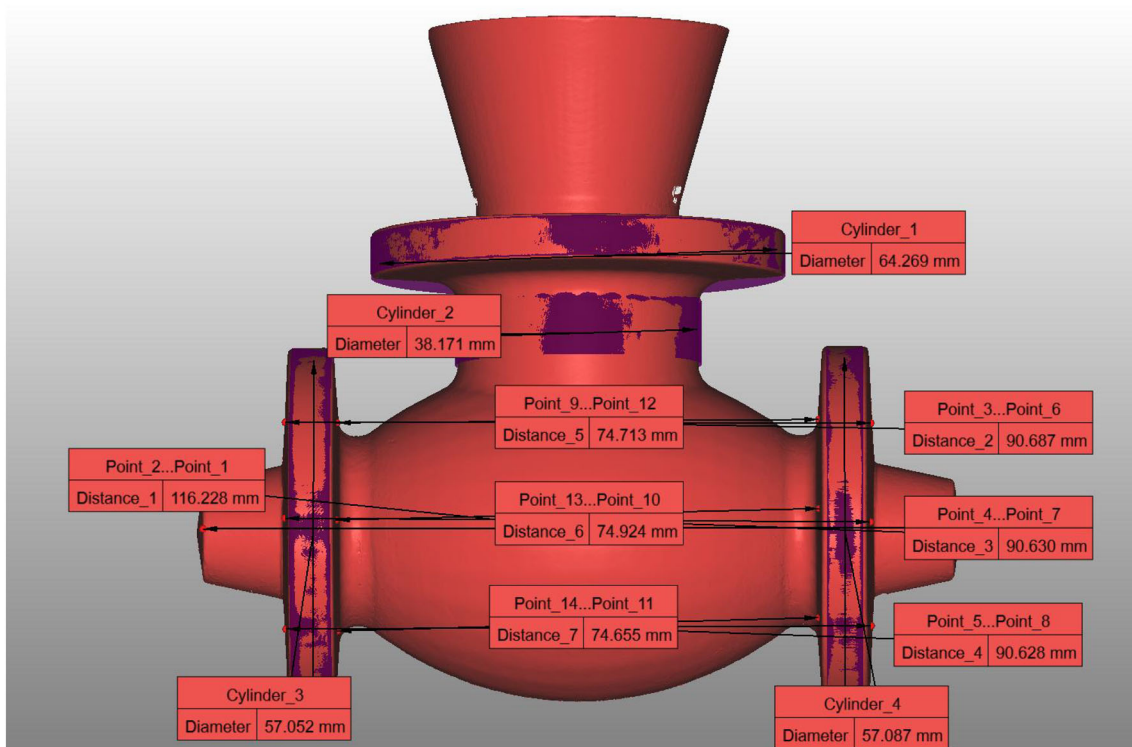


**Figure 5. 3D scan of the metal pattern used in this study along with some marked measurement.**

deemed sufficient to evaluate surface quality. For every casting, surface roughness was measured in 3 locations. One on the left flange, one on the right flange and one in the middle. 2mm-by-2mm area was inspected for the measurements. For each location, profile parameters  $R_a$  and  $R_z$  values were calculated, and a surface micrograph taken. Regions of pores or sand inclusions were carefully avoided while selecting each 2mm-by-2mm area. It is also possible to calculate surface texture parameters which quantify surfaces from an area viewpoint rather than line profile viewpoint (for example,  $R_a$  and  $R_z$ ). The  $S_a$  parameter is the closest to the  $R_a$  parameter, although they are fundamentally different. However, if the number of  $R_a$  values averaged increases, it tends to be closer to the  $S_a$  parameter, as reported in.<sup>32</sup> The profilometer software(Vision64) provides an  $R_a$  reading which is an average of roughness of the entire region being measured, hence the  $R_a$  values reported in this study are also very close approximation of  $S_a$  parameters.

Since the area of measurement does not lie in a planar surface, a compensation is required. In case of castings, even planar surface by design could deviate due to mold wall displacement and shrinkage differences.<sup>30</sup> In this study, the built-in function of vision 64 software was used for this compensation, which converts any curvature to a planar surface before roughness calculation. Roughness parameters were then noted as reported by the software.

## Results

The base properties of the sands used in this study are given in Table 4, while Figure 6 shows the sieve distribution and sand micrographs are shown in Figure 7. Density assumptions used for calculation of specific surface area were, silica: 2.65 g/cm<sup>3</sup>, sintered bauxite: 3.3 g/cm<sup>3</sup> and Cerabeads: 2.9 g/cm<sup>3</sup>. Shape assumptions used are shown in Table 4.

CB 400 has almost 3 times the permeability of silica sand due to their large grain size and very uniform circular shape. CB 400 had similar bulk density to silica while sintered Bauxite was much heavier. Sintered Bauxite had a very small negative loss on ignition, which means it gains slight weight due to oxidation.

## Mold Tests

Figure 8 shows the bending strength achieved with the different binder and sand types. Binder A produced the highest bending strength with all types of sand. Specifically, sintered Bauxite and Binder A produced bending strength as high as 448.5 N/cm<sup>2</sup>. For any particular binder type, CB 400 had the least strength. This was anticipated as CB 400 produced low strengths with organic binders as well.<sup>26</sup> Binder E produced intermediary results with all sand types.

**Table 4. Base Properties of the Sands Used in the Study**

	Mean particle size	AFS GFN	Grain Shape	Bulk Density (g/cm <sup>3</sup> )	Permeability	Moisture content (%)	LOI (%)	Specific Surface Area (cm <sup>2</sup> /g)
Silica	240 μm	62.8	Sub-angular	1.48	90-100	0.035	0.20	153.3
Sintered Bauxite	300 μm	51.1	Rounded	1.99	103-106	0.011	-0.01	85.9
Cerabeads 400	380 μm	40.8	Rounded, compound	1.49	300-330	0.013	0.15	77.0

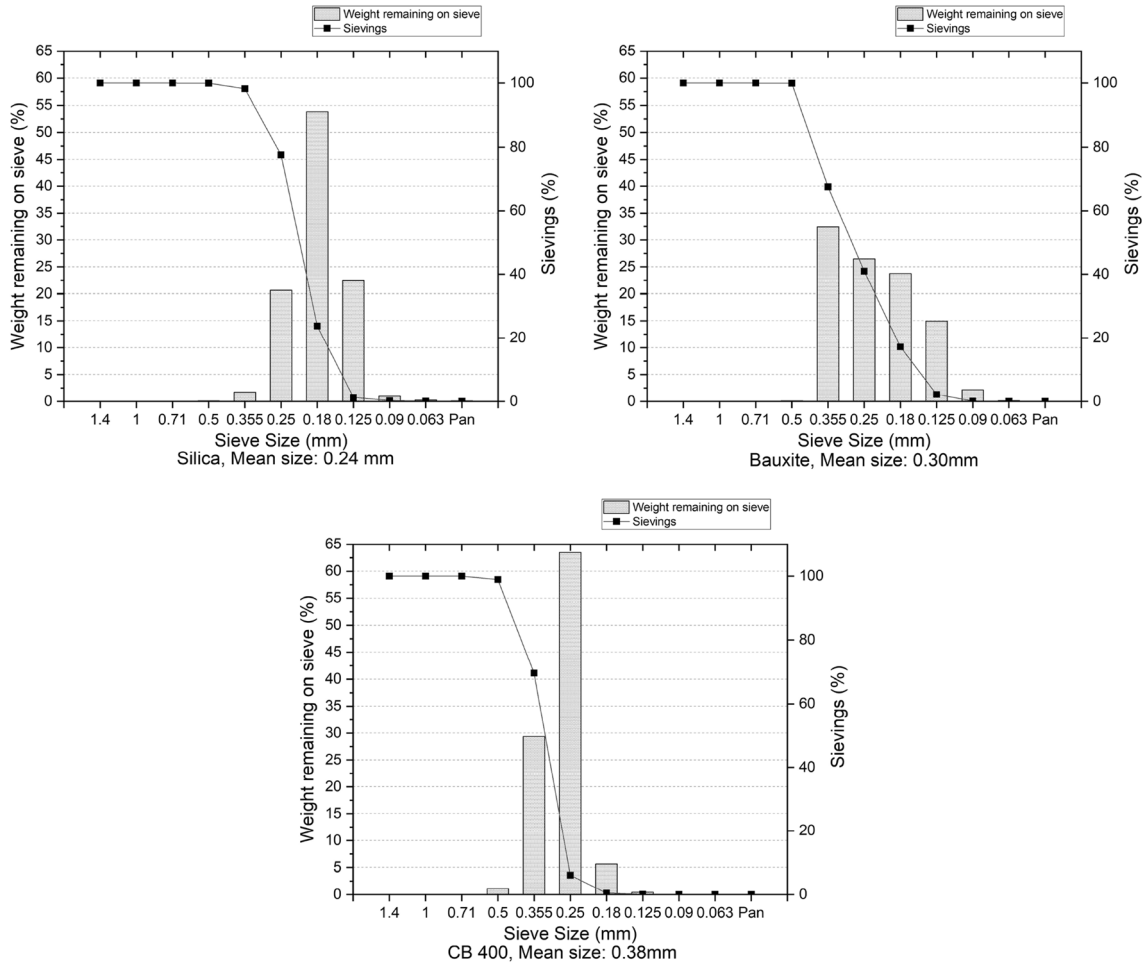


**Figure 6. Sieve distribution of the 3 sands used.**

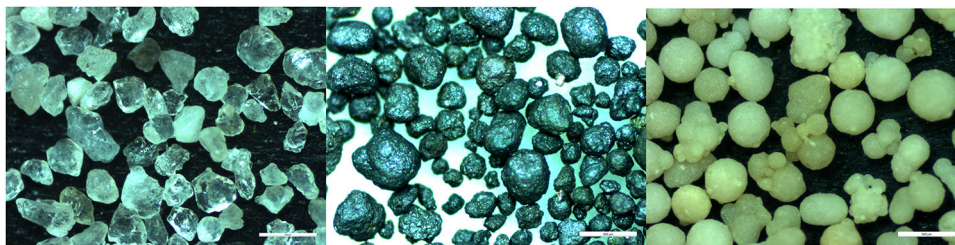


**Figure 7. Sand micrograph. On the left: Silica, center: Sintered Bauxite, right: Cerabeads 400.**

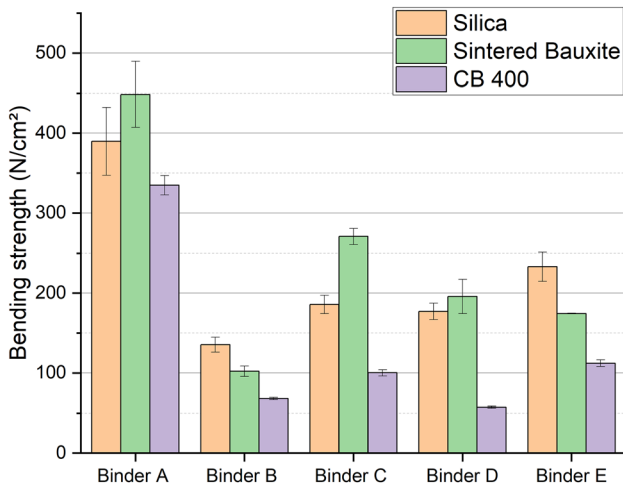


**Figure 8. Bending strength of molds made from inorganic binders and three types of sand.**

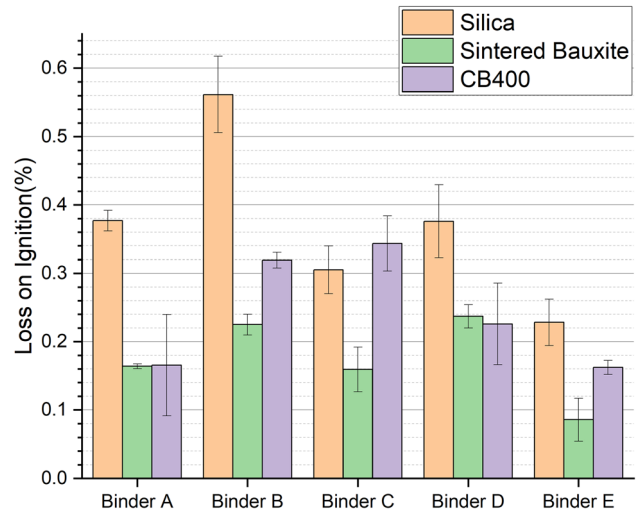


**Figure 10. Loss on ignition of test bars made from inorganic binders and three types of sand.**

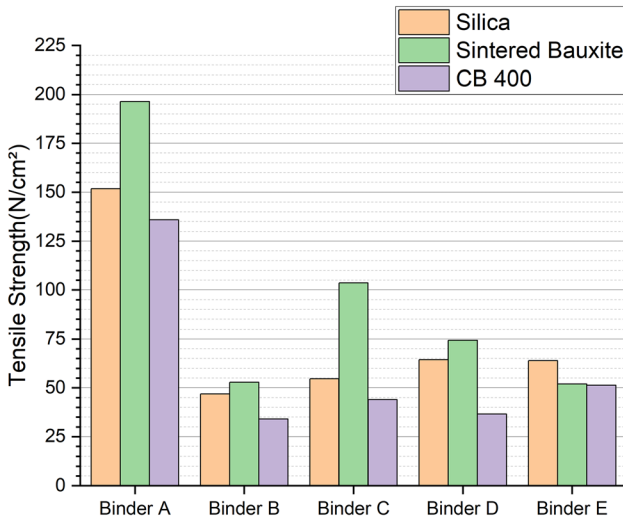


**Figure 9. Tensile strength of molds made from inorganic binders and three types of sand.**

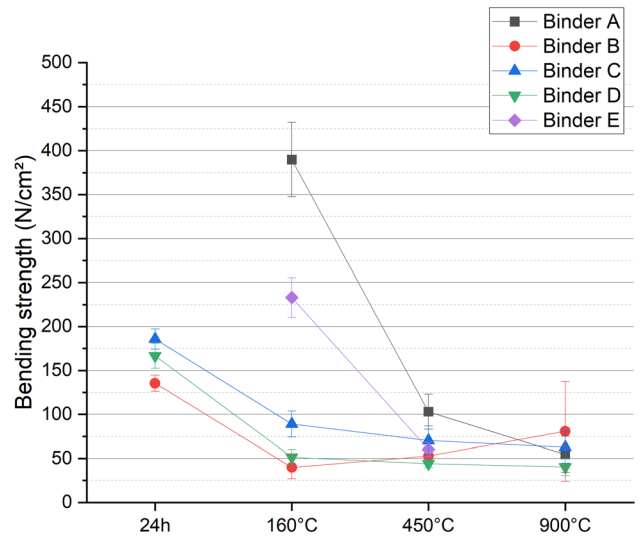


**Figure 11. Residual bending strength of inorganic binders with silica sand.**

Tensile strengths achieved with the different sand and binder types are shown in Figure 9. Like with bending strength results, the highest tensile strength is achieved with the combination of sintered Bauxite and liquid silicate. All three sands had tensile strength above 50 N/cm<sup>2</sup>. With all sand types, Binder B produced the least strength as was seen with bending strength. Except for Binder E, all other binders produced the highest tensile strength with sintered Bauxite sand.

For all inorganic binder types, the loss on ignition was less than what would be expected with organic binders as can be seen in Figure 10. Powder silicate and sintered Bauxite had the least loss on ignition, while silica and ester-cured liquid silicate (Binder B) had the highest loss on ignition. Except binder D, sintered Bauxite had the lowest loss on ignition. Bending strength and loss on ignition achieved



**Figure 12. Cracks developed in test bars when Sil-E test bars were heated to 900 °C.**

using phenolic and furan binder with different sands could be found in.<sup>26</sup>

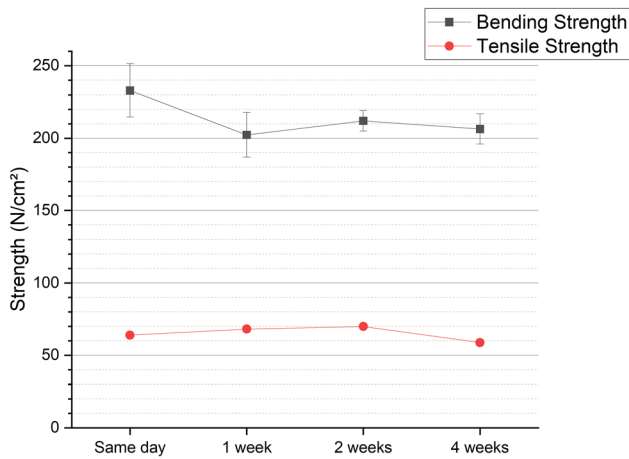


**Figure 13.** Strength obtained after storing silica sand and Binder E (solid silicates) as a mixture in closed containers.

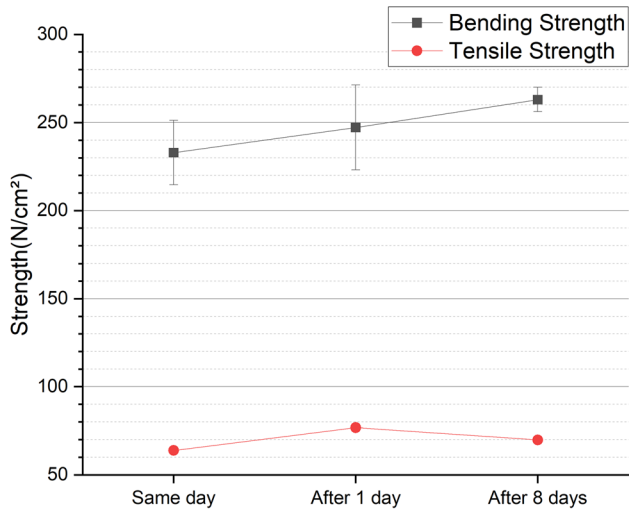


**Figure 14.** Strength obtained after storing silica sand and Binder E (solid silicates) as mixture open to air.

Figure 11 shows the residual mold strength of the inorganic molds at different temperatures. All the binders follow a similar profile of residual bending strength with temperature. It gradually decreases at 450 °C and further reduction in 900 °C. No strength could be measured for powder silicate at 900 °C. The heated test bars developed cracks and broke before they could be moved to the tester, as shown in Figure 12. For Binder B, successive increase in residual strength was noticed after 160 °C.

The effect of storing the solid silicate in closed containers is shown in Figure 13. The bending strength remains above 200 N/cm<sup>2</sup> over the period of 4 weeks while tensile strength remains above 50 N/cm<sup>2</sup>. This confirms that there is not much loss in strength if the powder silicate (Binder E) is kept in mixed form with silica sand up to 4 weeks before use. Storage in open containers was also studied, results shown in Figure 14.



**Figure 15.** On the left Sil-F casting and on the right Sil-A casting.



**Figure 16.** On the left Sil-D casting and on the right Sil-E casting.



**Figure 17.** On the left Bx-A casting and on the right Sil-Bx-E casting.

Bending strength increased after 1 day, and even more after 8 days. All tensile strength values registered were above 60 N/cm<sup>2</sup>.

### Casting Trials

Figures 15, 16, and 17 show select castings with visible differences in surface quality.

### Dimension Changes and Mesh-to-Mesh Analysis

For mesh-to-mesh analysis, the two extremes of the scale used were -1.00 (blue) mm to +1.00 mm (red). The software tracks differences in pattern and casting produced in this range after a best-fit alignment of the separate scans. The blue color corresponds to a place where the casting is smaller than the pattern, and red color to place where the casting is bigger than the pattern and with other gradual

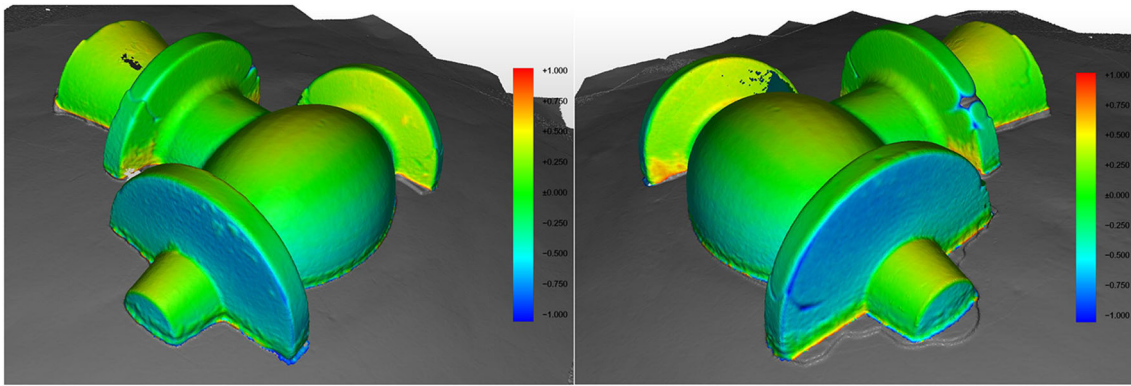


**Figure 18. Mesh-to-mesh analysis of casting obtained with Sil-F(silica and phenol mold) combination.**

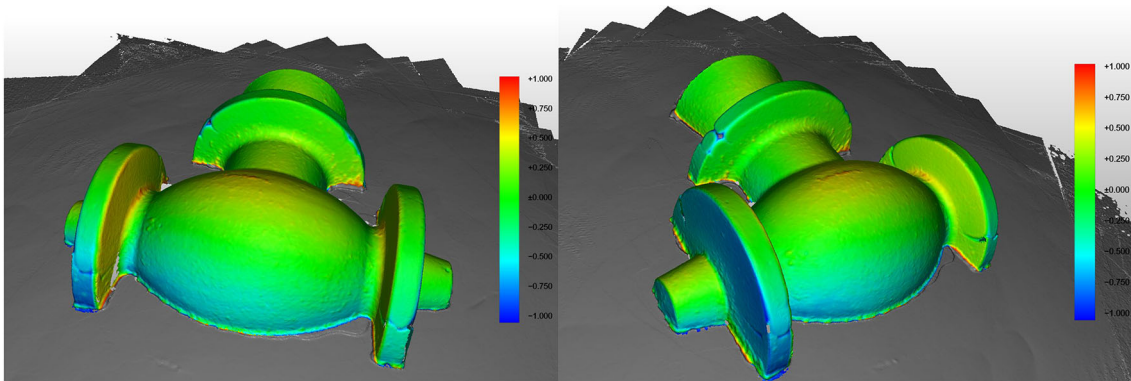


**Figure 19. Mesh-to-mesh analysis of casting obtained with Sil-C.**

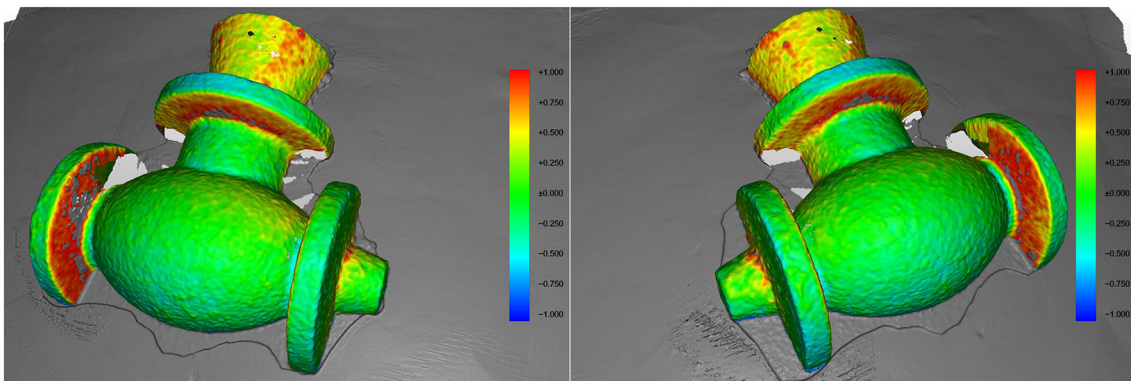


**Figure 20. Mesh-to-mesh analysis of casting obtained with Sil-E.**

changes in color in between as shown in Figure 18 for Sil-F casting. With Sil-F combination contractions could be seen on the outsides of both the flanges. While slight expansion is noticed to areas on both flanges on the inside. This is the expected casting contraction. Rest of the part remained within green to yellow zone. Comparable results were also obtained with Sil-G (silica furan) combination mold. Compared to this, Binder D showed less contraction on the outside. With Binder C, although the outside showed similar contraction, the inside of the flanges showed expansion compared to the pattern, as shown in Figure 19.

With Binder E, there is less contraction on the outside. Stark contrast is obtained with the powder sample as shown in Figure 20. There is much larger deviation on the inside of both flanges and small contractions can be seen on the top of the top flange. The situation is much improved both in terms of surface roughness and deviations in mesh-to-mesh comparison when a mold release agent was used with Binder E (Combination Sil-EMR).

To track a generalized change in dimensions from pattern to mold and mold to casting, specific distances were

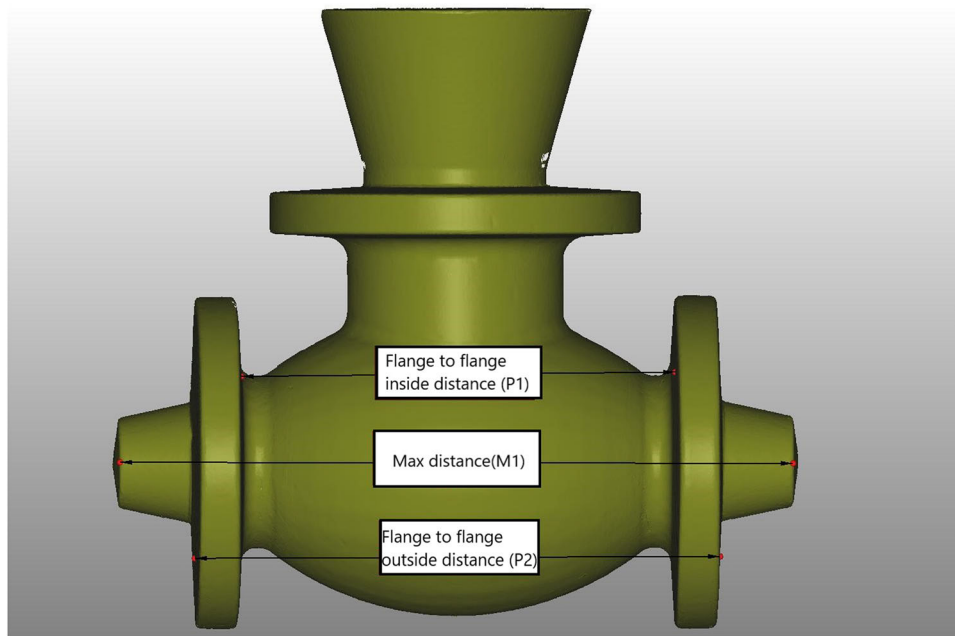


**Figure 21. Dimensions used in the tracking of dimensional change from pattern to final castings**

**Table 5. Dimensional Changes Calculated Using Inside Flange-to-Flange Distance (P1)**

	Pattern to mold	Mold to casting	Pattern to casting
Sil-A	-0.525 %	-0.365 %	-0.889 %
Sil-B	-0.428 %	-0.684 %	-1.109 %
Sil-C	-0.633 %	-0.375 %	-1.006 %
Sil-D	-0.275 %	-0.784 %	-1.057 %
Sil-E	-1.260 %	-1.312 %	-2.556 %
Sil-EMR	-0.430 %	-1.046 %	-1.472 %
Sil-F	0.189 %	-1.079 %	-0.892 %
Sil-G	-0.568 %	-0.343 %	-0.909 %
Bx-A	-1.766 %	-0.310 %	-2.070 %
Bx-E	-1.367 %	-0.785 %	-2.141 %
Sil-Bx-A	-0.739 %	-0.529 %	-1.264 %
Sil-Bx-E	-1.296 %	-0.543 %	-1.832 %

**Table 6. Dimensional Changes Calculated Using Outside Flange-to-Flange (P2) and Max Distance (M1)**

	Pattern to mold	Mold to casting	Pattern to casting
Sil-A	-0.007 %	-0.553 %	-0.561 %
Sil-B	-0.167 %	-0.769 %	-0.935 %
Sil-C	-0.070 %	-1.015 %	-1.084 %
Sil-D	-0.036 %	-0.786 %	-0.822 %
Sil-E	0.836 %	-0.506 %	0.325 %
Sil-EMR	0.486 %	-0.826 %	-0.344 %
Sil-F	-0.049 %	-1.131 %	-1.181 %
Sil-G	0.030 %	-1.051 %	-1.021 %
Bx-A	0.477 %	-0.144 %	0.332 %
Bx-E	0.769 %	-0.607 %	0.158 %
Sil-Bx-A	0.382 %	-0.472 %	-0.091 %
Sil-Bx-E	0.979 %	-0.760 %	0.210 %

measured as shown in Figure 21. Three different values are taken for P1 across the flange and averaged. Same is done with P2 measurement. Only one value is measured for M1. Tracking the dimensional change was done in two stages: one with only P1 as shown in Table 5 and the other with an average of P2 and M1 as shown in Table 6.

With respect to the inside flange-to-flange distance, a pattern to casting change between -0.89 and -1.11% was seen with all self-setting systems (both inorganic and organic). A high percentage change was seen for Sil-E and

Sil-EMR. Sil-A showed a change of -0.9%. The highest was seen with the sintered Bauxite (Bx-A and Bx-E), at slightly more than -2%.

For P2 and M1, the pattern to casting change stayed between -0.82 and -1.18% for the self-setting systems. With Sil-A, it was -0.561%, Sil-E at 0.325%, and Sil-EMR -0.34%. Both sintered Bauxite systems had seen positive increase of +0.33% (Bx-A) and +0.16% (Bx-E).

**Table 7. Surface Roughness Values of the Castings Obtained**

	Left flange		Middle		Right flange		General casting defects observed
	$R_a$ ( $\mu\text{m}$ )	$R_z$ ( $\mu\text{m}$ )	$R_a$ ( $\mu\text{m}$ )	$R_z$ ( $\mu\text{m}$ )	$R_a$ ( $\mu\text{m}$ )	$R_z$ ( $\mu\text{m}$ )	
Pattern	6.66	69.30	4.22	49.32	3.90	68.69	
Sil-A	16.80	136.64	28.74	194.45	13.54	105.86	
Sil-B	32.66	237.30	17.29	161.44	13.48	98.47	
Sil-C	9.23	83.94	14.51	116.27	12.38	100.49	
Sil-D	17.25	197.35	7.67	88.56	10.93	87.23	
Sil-E	44.37	304.32	68.59	418.64	53.41	390.75	
Sil-EMR	49.16	281.27	14.39	142.24	47.17	318.64	Minor penetration on left core print
Sil-F	10.98	80.33	7.41	58.67	5.78	46.53	
Sil-G	12.02	100.13	10.93	73.25	8.58	75.30	
Bx-A	31.74	238.48	23.26	192.93	18.63	173.61	Minor penetration on right core print
Bx-E	52.85	387.30	77.33	489.18	55.52	394.92	Material penetration on left flange
Sil-Bx-A	18.34	163.34	38.01	249.20	29.58	204.15	
Sil-Bx-E	34.99	241.08	22.98	218.62	26.40 (Top flange)	263.75 (Top flange)	Material penetration on right flange

**Surface Roughness and Integrity Analysis**

Surface roughness can be visually inspected and compared; differences evident in Figures 15, 16, and 17. Differences can also be seen in 3D scan results of the castings when the differences are relatively large. However, to quantify the surface roughness of  $R_a$  (arithmetic average of absolute values of profile height deviations from mean line) and  $R_z$  (average value of absolute values of heights of highest-profile peaks and depths of deepest valleys) were measured. The results are given in Table 7. Additionally, descriptions of general casting defects observed are noted in the table. Some minor cold shuts were seen in the flange areas of the analyzed castings. These are not listed in the table as those are related to melt flow rather than mold characteristics. Average of 3  $R_a$  measurement for each casting is shown in Figure 22.

The pattern in use had an average  $R_a$  of 4.92 $\mu\text{m}$ . The best surface finish was achieved with phenolic binder (Combination Sil-F) at 8.06  $\mu\text{m}$ , followed very closely by the furan binder (Combination Sil-G) at 10.51  $\mu\text{m}$ . Commercially used ester-cured sodium silicate (Sil-C) produced an  $R_a$  of 12.04  $\mu\text{m}$  and that by geopolymer (Sil-D) 11.95  $\mu\text{m}$ . Very high surface roughness was seen with Sil-E at 55.45  $\mu\text{m}$ . This reduced to 36.91  $\mu\text{m}$  when a mold release agent was used (Sil-EMR). The worst surface roughness was seen with Bx-E (61.9  $\mu\text{m}$ ). However, when 50% of silica and 50% of sintered Bauxite was used (Combination Sil-Bx-E), the average surface roughness was 28.12  $\mu\text{m}$ . This was much less than when only either silica or sintered Bauxite was used with Binder E. Some surface micrographs are shown in Figure 23.

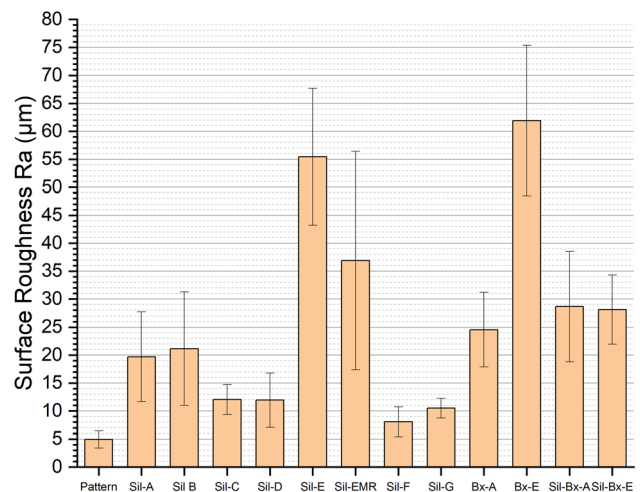
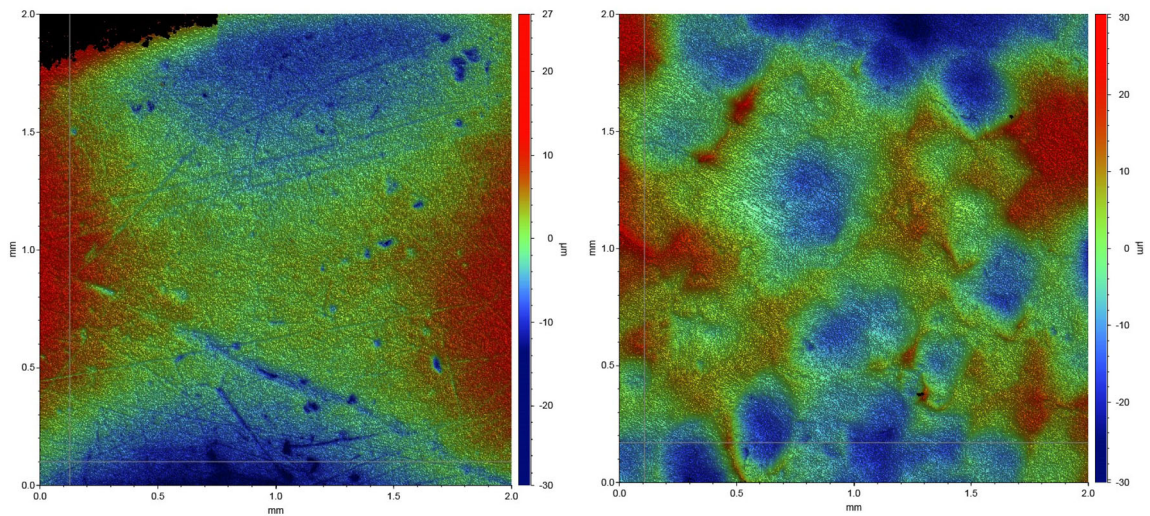


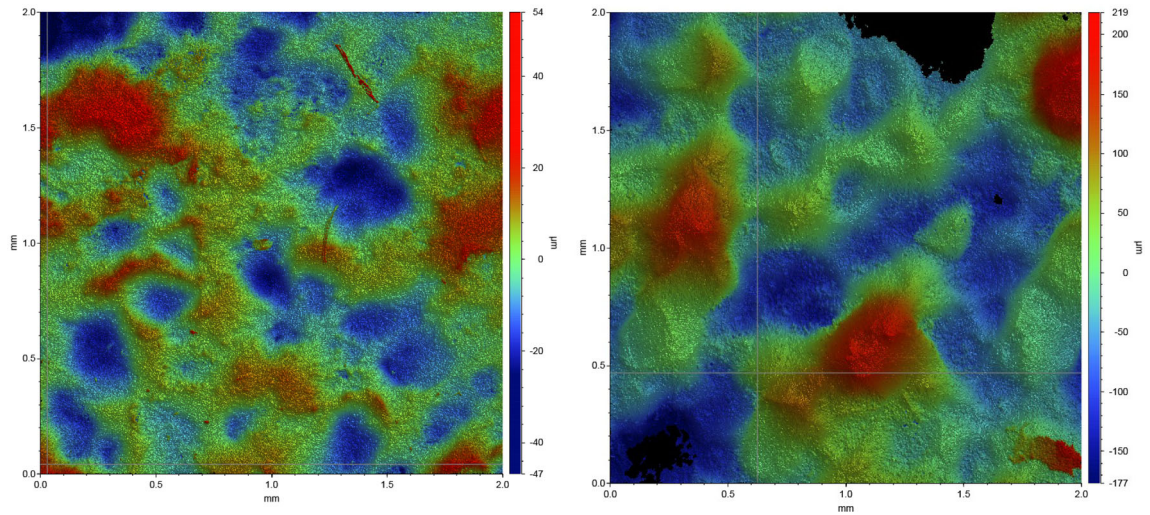
**Figure 22. Average of 3  $R_a$  readings.**

In order to have a better understanding for the high surface roughness value of Sil-E combination, another small test was done. Sil-E mold was made again but this time with a different 3D-printed plastic pattern (thermally resistant up to 200°C). The shape of this pattern was slightly different from the original metal pattern used, but similar in nature. Figure 24 shows the 3D scan of original Sil-E mold, Figure 25 shows the one with 3D-printed pattern. The improvement in surface roughness is quite evident with the new pattern, both visually and also in the 3D scans of the molds.



Pattern Middle. Ra: 4.23  $\mu\text{m}$

Sil-F middle. Ra: 7.41  $\mu\text{m}$ .



Sil-D Middle. Ra: 7.67  $\mu\text{m}$

Sil-E right flange. Ra: 53.41  $\mu\text{m}$

**Figure 23.** Some select surface micrographs are shown.

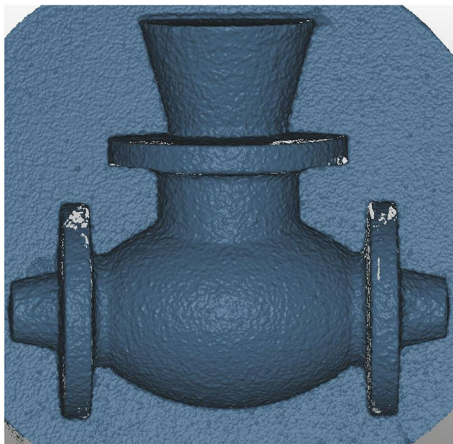


**Figure 24.** 3D scan of Sil-E mold made with metal pattern.



**Figure 25.** 3D scan of Sil-E mold made with 3D-printed thermal-resistant plastic pattern.

## Discussion

The bending strength achieved in all the different forms of inorganic binders was in acceptable range for foundry use, although the ester-cured sodium silicate was on the lower ranges. However, by altering the amount of binders and/or hardeners the achievable strength can be altered even for specific purposes. As collapsibility is an issue with inorganic binders, residual bending strength was also investigated in this study. All the inorganic binders exhibited a similar trend in residual strength, strength decreasing with increasing temperature but does not fall to zero. Only Binder B showed an increase in residual strength at 450 and 900 °C. Due to binder burnout, organic binders do not retain their strength like inorganic ones do, resulting in their excellent collapsibility. As an example, the tensile strength of furan (1.2%) and silica goes almost zero already at 400 °C.<sup>33</sup> The loss on ignition of inorganic binders with all types of sand was quite small as expected. All organic binders exhibit a much higher loss on ignition as could be seen in.<sup>26</sup> As anticipated, Binder B-system has higher loss on ignition than the fully inorganic binders, the ester-cured sodium silicate being a semi-inorganic system.

Pattern removal was the easiest with the organic systems (Binders F and G). Inorganic binders C and D were also good with pattern release. However, in all the heat-hardened systems pattern removal was challenging. Also, if patterns must be kept inside molds for the whole hardening process, then pattern and mold material can expand or contract at different rates making pattern removal even more challenging. Easy pattern release is also quite important so that minimal damage is made to the mold. The most difficult pattern release was experienced with Binder E in this study.

The expected casting contraction for unannealed spheroidal gray cast iron is about 1.2% (p. 41 Annex B).<sup>34</sup> This is given as a total change in pattern to casting. In this study, the overall pattern to casting change lied between -0.82% and -1.18% for all the self-setting systems (where heat was not used for hardening). A range of changes were noticed for the heat-hardened ones. For example, if the inside flange-to-flange distance is considered (P1), Sil-E had a pattern to mold change of -1.26%. One possible reason could be, as the mold tended to stick to the pattern, some sand was scratched off when taking the pattern out, resulting in a decrease in the inside flange-to-flange distance. When the release agent was used in Sil-EMR, this change came down to -0.43%. The same was also evident with the outside flange-to-flange distance and max distance (P2 and M1), where scratching layers of sand actually increases this distance. Hence, pattern to mold change of +0.84% was seen with Sil-E and this change came down to +0.49% when a mold release agent was used (Sil-EMR). The high dimensional changes in castings with sintered Bauxite sand could be due to their larger size and size

distribution, thus any scratch of layer produces larger changes. Another reason could also be due to small penetrations at M1 measurement site. In either way, separate more extensive research is required to establish the exact allowance needed with these binder and sand types.

There were both encouraging results and challenges concerning solid silicates (Binder E). The strength produced with solid silicates was in acceptable range, if not better in some cases, than some of the ester-cured silicates. The loss on ignition was also low, in fact the lowest loss on ignition noted in this study was recorded with the combination of sintered Bauxite and solid silicates. Very encouraging results were also noticed with the tests conducted for the storability of solid silicates and sand in a mixed form. Such mixture was stored in a closed container, tested after storage periods up to 4 weeks, and not much deterioration in strength was noticed. On the contrary, when stored open to air, strength increased within the test trial period of up to 8 days. The moisture in air has potentially helped in improving dissolution of the sodium silicate powder. More tests should be conducted to see how long such mixtures can be stored in open air before losing binding properties or starting to clump. This means there is potential for foundry practice where sand could be bought, or made into mixtures, or coated with sodium silicate as one product and foundries only supply water for the hardening. It should also be emphasized that the mass of solid silicate used in each batch was only 14.11g, compared to the 51g of liquid silicate or even to the 42.5 g of Binder C (Commercial brand of ester-cured sodium silicate). This also demonstrates the ease of transportation and storage of solid silicates.

The surface roughness ( $R_a$ ) of a small-medium sand casting is expected to be up to 12.5  $\mu\text{m}$ , in medium-large casting up to 25  $\mu\text{m}$  and that of large castings up to 50  $\mu\text{m}$ .<sup>35</sup> In this study, the best surface finish was obtained with organic binders F and G (Average  $R_a$  8.06  $\mu\text{m}$  and 10.51  $\mu\text{m}$ , respectively). Even though Binder A and B did not produce excellent surface finish ( $R_a$  around 20  $\mu\text{m}$ ), commercially available ester-cured sodium silicate Binder C produced quite comparable results to the organic binders. Geopolymer binder also achieved similar result as Binder C. It is thus to be expected that with more research, inorganic binders should be able to match the surface roughness achieved with organic binders. The highest surface roughness was achieved with Binder E. Both Sil-E and Bx-E castings having  $R_a$  values more than 50 $\mu\text{m}$ . This issue is discussed in more detail in the following section.

One contributing factor of high surface roughness of Sil-E castings could be because powder silicate tended to stick to the metal pattern. This makes pattern removal very difficult, also causing the surface of the mold to be damaged and resulting in high surface roughness values with Binder E. However, five aspects should be discussed here. Firstly,

it must be emphasized that the unmodified liquid sodium silicate also produced rough surfaces in this study. Commercial silicate binders have improved on this through modifications and additives, as demonstrated by Binder C. Similar improvements should be possible in case of powder silicate. Secondly, the use of mold release agent did improve the surface roughness to some extent (Sil-EMR).  $R_a$  improved from 55.46 to 36.91  $\mu\text{m}$ . Thirdly, the mold with a mixture of 50% sintered Bauxite and 50% silica had a smaller surface roughness than when either silica or sintered Bauxite was used alone. This indicates potential in mold aggregate mixtures. Fourthly, the quick test of making Sil-E mold with a 3D-printed pattern had shown to be of much smoother surface than the original Sil-E mold (Figures 24 and 25). The pattern released much better and it did not stick to the mold. This leads the authors to believe that surface finish could be much improved if pattern release could be improved with Binder E. Fifthly, in the case of 3D printing of sand mold using powder silicates where the sand is premixed with the powder and water is jetted through the print heads, such issues do not exist as there is no pattern to remove and hence no issue of sand sticking to the pattern. Therefore, although the powder silicate binder tested here is not ready for foundry use as is, with research, binder modification, coatings, additives, pattern material improvement these have the potential to be a main-line form of inorganic binder for foundry use in the future.

One of the challenges of sodium silicate binder is the difficulty of sand reclamation after use.<sup>36</sup> Remaining sodium silicate are not decomposed or burned out in the casting process but instead they form a sodium silicate gel.<sup>37</sup> This has low melting point and strong bond strength with the sand. Residual binder and salt on the sand absorb water easily which makes dry reclamation difficult. However, most of the residues (sodium silicate, esters, and salts formed) are soluble in water. Hence, a wet reclaiming process can produce very good quality reclaimed sand. However, if a large amount of water is required in the wet reclamation process, large quantity of sewage discharge then produces secondary pollution.<sup>38</sup> Solving this reclamation issue is vital as not doing so beats the purpose of using environmentally friendly binder in the first place. An environmentally friendly binder would be no more sustainable than organic ones if foundries have to use significantly more virgin sand mined from continually diminishing natural reserves.

### Future Work

- Investigating applicable pattern materials and allowances for dimensional changes with inorganic binders.

- Investigating different ways of physical hardening of sodium silicate: furnace heating, microwave, induction, etc.
- Investigating parameters for three-dimensional printing with solid silicates.
- Investigating different coatings for improving castings, for example to improve surface quality.

### Conclusion

Re-emergence of inorganic binders offers solutions to global sustainability challenges. The challenges are clear to see but there are also significant advantages that foundries can exploit for their benefit. The principal advantage being environmental, while additional benefits like savings in binder purchase, tooling, etc. All the inorganic binders tested here demonstrated good mold strength, maybe even too high in some cases. The loss on ignition values were also very good compared to organic binders. However, the surface finish achieved with organic binders is still superior to inorganic ones, although the commercially available sodium silicate and geopolymers are very close. It is possible to obtain castings through solid sodium silicates, however the surface roughness issues need to be solved before widespread use in foundries is possible. Very encouraging results were obtained with the storage of solid silicates and sand as a mixture. As the manufacturing world is seeking more sustainability and environmental laws getting ever stricter, inorganic binders might become the new norm of foundry use across the globe.

### Acknowledgement

The authors acknowledge Soilikki Kotanen for her expertise with binders and sourcing of binders and TAKK foundry and personnel for their help with the casting trials.

### Funding

Open Access funding provided by Aalto University. This research was funded by Aalto University and Business Finland. The authors have no relevant financial or non-financial interests to disclose.

### Open Access

This article is licensed under a Creative Commons Attribution 4.0 International License, which permits use, sharing, adaptation, distribution and reproduction in any medium or format, as long as you give appropriate credit to the original author(s) and the source, provide a link to the Creative Commons licence, and indicate if changes were made. The images or other third party material in this article are included in the article's Creative Commons licence, unless indicated otherwise in a credit line to the material. If material is not included in the article's Creative

Commons licence and your intended use is not permitted by statutory regulation or exceeds the permitted use, you will need to obtain permission directly from the copyright holder. To view a copy of this licence, visit <http://creativecommons.org/licenses/by/4.0/>.

## REFERENCES

1. H. Polzin, *Inorganic binders: for mould and core production in the foundry*, 1st ed. Fachverlag Schiele & Schön GmbH, (2014)
2. M. Holtzer and A. Kmita, *Mold and Core Sands in Metalcasting: Chemistry and Ecology: Sustainable Development*. Cham: Springer International Publishing (2020). [https://doi.org/10.1007/978-3-030-53210-9\\_4](https://doi.org/10.1007/978-3-030-53210-9_4).
3. J. R. Brown, Ed., *Foseco Ferrous Foundryman's Handbook*, 11th ed. Elsevier, (2000)
4. J.T. Fox, F.S. Cannon, N.R. Brown, H. Huang, J.C. Furness, Comparison of a new, green foundry binder with conventional foundry binders. *Int. J. Adhes. Adhes.* (2012). <https://doi.org/10.1016/j.ijadhadh.2011.11.011>
5. A. Kmita, C. Fischer, K. Hodor, M. Holtzer, A. Rocznik, Thermal decomposition of foundry resins: a determination of organic products by thermogravimetry–gas chromatography–mass spectrometry (TG–GC–MS). *Arab. J. Chem.* **11**(3), 380–387 (2018). <https://doi.org/10.1016/j.arabjc.2016.11.003>
6. M. Holtzer, A. Kmita, S. Żymankowska-Kumon, R. Dańko, Influence of the hardener on the emission of harmful substances from moulding sands with Furan resin in the pyrolysis process. *Arch. Foundry Eng.* **16**(1), 107–111 (2016). <https://doi.org/10.1515/afe-2016-0012>
7. H. Zhang, H. Zhao, K. Zheng, X. Li, G. Liu, Y. Wang, Diminishing hazardous air pollutant emissions from pyrolysis of furan no-bake binders using methanesulfonic acid as the binder catalyst. *J. Therm. Anal. Calorim.* **116**(1), 373–381 (2014). <https://doi.org/10.1007/s10973-013-3553-x>
8. N. Bakhiya, K.E. Appel, Toxicity and carcinogenicity of furan in human diet. *Arch. Toxicol.* (2010). <https://doi.org/10.1007/s00204-010-0531-y>
9. L. Zaretskiy, Modified silicate binders new developments and applications. *Int. J. Met.* (2016). <https://doi.org/10.1007/s40962-015-0005-3>
10. A. Fortini, M. Merlin, G. Raminella, A comparative analysis on organic and inorganic core binders for a gravity diecasting alloy component. *Int. J. Met.* **16**, 674–688 (2022). <https://doi.org/10.1007/s40962-021-00628-1>
11. J. Campbell, *Complete Casting Handbook*, 1st ed. Elsevier Ltd., (2011)
12. K. Granat, D. Nowak, M. Pigiel, M. Stachowicz, R. Wikiera, The influence of hardening method on basic properties of water glass molding sands. *Visn. Chmel'nickogo Nac. Univ.* **1**(4), 98–104 (2007)
13. A. Malachowska, M. Stachowicz, K. Granat, Innovative microwave hardening of water-glass containing sandmixes in technical-economic approach. *Arch. Foundry Eng.* **12**(1), 75–80 (2012). <https://doi.org/10.2478/v10266-012-0015-z>
14. P. Jelinek, Binding systems of foundry moulding sands (in Czech) (2004)
15. S.M. Dobosz, K. Major-Gabryś, M. Hosadyna, New look at the process of reclamation of moulding sands. *Arch. Foundry Eng.* **12**(3), 19–24 (2012). <https://doi.org/10.2478/v10266-012-0075-0>
16. J. L. Lewandowski, Materials for foundry moulds (1997)
17. A. Kmita, B. Hutera, Effect of water glass modification on its viscosity and wettability of quartz grains. *Arch. Foundry Eng.* **12**(3), 59–62 (2012). <https://doi.org/10.2478/v10266-012-0082-1>
18. F. Xin, W. Liu, L. Song, Y. Li, Modification of inorganic binder used for sand core-making in foundry practice. *China Foundry* **17**(5), 341–346 (2020). <https://doi.org/10.1007/s41230-020-0018-2>
19. L. Zaretskiy, Hydrous solid silicates in new foundry binders. *Int. J. Met.* **12**(2), 275–291 (2018). <https://doi.org/10.1007/s40962-017-0155-6>
20. R. Ramakrishnan, B. Griebel, W. Volk, D. Günther and J. Günther, 3D printing of inorganic sand moulds for casting applications (2014). <https://doi.org/10.4028/www.scientific.net/AMR.1018.441>.
21. I. Vaskova, M. Coney, M. Hrubovčáková, Technological properties of moulding sand with geopolymer binder for aluminum casting. *Arch. Foundry Eng.* **18**(4), 45–49 (2018). <https://doi.org/10.24425/123631>
22. M. Vykoukal, A. Burian, M. Přerovská, GEOPOL®. the innovated environment friendly inorganic binder system. *Arch. Foundry Eng.* **19**(1), 109–116 (2019). <https://doi.org/10.24425/afe.2019.127103>
23. M. Holtzer, D. Drożyński, A. Bobrowski, W. Plaza, Influence of binding rates on strength properties of moulding sands with the geopol binder. *Arch. Foundry Eng.* **14**(1), 37–40 (2014). <https://doi.org/10.2478/afe-2014-0009>
24. F. Pezarski, E. Smoluchowska, I. Izdebska-Szanda, Application of geopolymer binder in manufacturing of casting from ferrous alloys. *Trans. Foundry Res. Inst.* **2**, 19–34 (2008). <https://doi.org/10.7356/iod.2008.7>
25. M. Vykoukal, A. Burian, M. Přerovská, T. Bajer, J. Beño, Gas evolution of GEOPOL® W sand mixture and comparison with organic binders. *Arch. Foundry Eng.* **19**(2), 49–54 (2019). <https://doi.org/10.24425/afe.2019.127115>
26. N. Anwar, T. Sappinen, K. Jalava, J. Orkas, Comparative experimental study of sand and binder for flowability and casting mold quality. *Adv. Powder Technol.* **32**(6), 1902–1910 (2021). <https://doi.org/10.1016/j.apt.2021.03.040>

27. American Foundry Society, *Mold & Core Test Handbook*, 4th ed. American Foundry Society, 2015.
28. A. D. Sarkar, *Mould & Core Material for the Steel Foundry*, 1st ed. Pergamon Press, 1967.
29. R. Tuttle, S. Ramrattan, L. Wells, As-cast surface characterization for steel using disk-shaped chemically bonded sand specimens. *Int. J. Met.* **15**(2), 382–390 (2021). <https://doi.org/10.1007/s40962-020-00520-4>
30. D.W. Schimpf, F.E. Peters, Variogram roughness method for casting surface characterization. *Int. J. Met.* **15**(1), 17–28 (2021). <https://doi.org/10.1007/s40962-020-00451-0>
31. D.W. Schimpf, F.E. Peters, 3D analysis of casting surface characterization based on the variogram roughness method. *Int. J. Met.* (2021). <https://doi.org/10.1007/s40962-021-00693-6>
32. H. T. Lancashire, A simulated comparison between profile and areal surface parameters: Ra as an estimate of Sa, pp. 1–9, 2017, [Online]. Available: <http://arxiv.org/abs/1708.02284>
33. F. Liu et al., Performance of resin bonded sand for magnesium alloy casting. *J. Manuf. Process.* **30**, 313–319 (2017). <https://doi.org/10.1016/j.jmapro.2017.10.002>
34. SFS-EN 12890 Founding. Pattern, pattern equipment and coreboxes for the production of sand moulds and cores. Finnish Standards Association, p. 45, 2000.
35. SFS-EN 1370 Founding. Examination of surface condition. Finnish Standards Association, 2011.
36. L. Wang, W. Jiang, F. Liu, Z. Fan, Investigation of parameters and mechanism of ultrasound-assisted wet reclamation of waste sodium silicate sands. *Int. J. Cast Met. Res.* (2018). <https://doi.org/10.1080/13640461.2017.1405543>
37. Z. Fan, N. Huang, H. Wang, X. Dong, Dry reusing and wet reclaiming of used sodium silicate sand. *China Foundry* **2**(1), 1–6 (2005)
38. W. Huafang, F. Zitian, Y. Shaoqiang, L. Fuchu, and L. Xuejie, Wet reclamation of sodium silicate used sand and biological treatment of its wastewater by *Nitzschia palea*, *China Foundry*, 2012.

**Publisher's Note** Springer Nature remains neutral with regard to jurisdictional claims in published maps and institutional affiliations.